VIII International Conference on Particle-Based Methods
PARTICLES 2023
U. Perego, M. Cremonesi, A. Franci (Eds)

SKIN LAYER FORMATION IN PLATE MODEL FOR COUPLED ANALYSIS OF INJECTION MOLDING PROCESS OF BONDED MAGNETS - PARTICLES 2023

Yohei UEMATSU[*1] , Katsuhiro HIRATA[*1], Fumikazu MIYASAKA[*1], Toya KITAMURA[*1] , Towa KIKUGAWA[*1]

[*1] Osaka University
9-1 Suita, Toyonaka, Osaka 560-0043, Japan
E-mail: info@osaka-u.ac.jp
Web page: https://www.osaka-u.ac.jp/en

Abstract. *The bonded magnet, which is formed by mixing magnet materials such as neodymium-based and ferrite-based materials with resin, has the characteristic of being able to be formed into small and complex shapes due to the resin being the binding material. It is used in small motors embedded in hard disk drives and motors for home appliances. The major methods for forming bonded magnets are compression molding and injection molding. In this study, injection molding is selected, which can easily apply to complex shape compared to compression molding. However, injection molding has the disadvantage of variability in density and magnetic properties of the molded products. This is due to the difficulty in observing the material flow, as the molding process progresses inside the mold and multiple processes occur simultaneously such as injection, compression, magnetization, and curing. Therefore, determining the optimal molding parameters for injection molding of bonded magnets requires numerous experimental trials. Based on the above, it is believed that predicting the behavior of resin inside the mold during the molding process using numerical simulation can provide guidelines for determining the optimal molding parameters. The authors have previously proposed a coupled analysis method of "fluid analysis and temperature analysis using MPS (Moving Particle Simulation) method, and magnetic field analysis using magnetic moment method." The objective of this study is to assess the solidification process of resin on the mold surface, utilizing a rectangular-shaped mold model.*

Keywords: bonded magnet, injection molding, meshless analysis method, particle method.

1 INTRODUCTION

Bonded magnets, which are molded by mixing neodymium or ferrite magnets such as Nd-Fe-B with resin, are used in small motors built into hard disk drives and motors for home appliances because the bonding material is resin, and can be molded into small and complex shapes [1]. Compression molding and injection molding are the main molding methods for bonded magnets. This study deals with injection molding, which offers a greater degree of freedom of shape than compression molding. However, injection molding has the disadvantage of causing variations in the density and magnetic properties of molded products. One of the reasons for the difficulty in controlling this variation is that the behavior of the injection molding process is not well understood. As a result, many trials are required to experimentally

determine the optimum parameters for injection molding of bonded magnets, making optimization difficult. To address this problem, a coupled analysis of the particle method [2]d the magnetic moment methods [3] proposed in a previous study [4]. However, the accuracy of the temperature analysis is low and room for improvement remains. The purpose of this paper is to propose an analytical model that takes into account heat conduction in the mold and to verify the validity and accuracy of the method through numerical analysis of the injection molding of bonded magnets.

2 ANALYSIS METHOD

To simulate the molding process of injection molding of bonded magnets, the following three coupled analyses are required.

- Fluid analysis to understand resin behavior
- Magnetic field analysis to understand magnetization distribution
- Temperature analysis to understand temperature changes due to heat dissipation

In this chapter, each of these analysis methods is described, followed by the coupling method.

2.1 Fluid analysis and temperature analysis

2.1.1 Fluid analysis

The governing equations for fluid analysis are the law of conservation of mass (Eq.1) and the law of conservation of momentum (Eq.2) for an incompressible fluid. where $\boldsymbol{u}$ is the velocity of the fluid, ρ is the density, $\boldsymbol{P}$ is the pressure, ν is the kinematic viscosity, $\boldsymbol{g}$ is the acceleration due to gravity, and $\boldsymbol{f}$ is the acceleration due to external forces. D/Dt represents the Lagrange differential operator, which is the time derivative from the point of calculation moving with the fluid. The time derivative is the time derivative as seen from the computational point moving with the fluid. In the calculation, it can be treated as a normal time derivative.

When the MPS method is used for fluid analysis, the particle number density becomes small near the surface, and the pressure distribution is easily disturbed. Therefore, in this analysis, the high-precision MPS method[5],[6],[7],[8] , which is an improved version of the MPS method, was used to solve this equation in order to suppress the turbulence in the pressure distribution.

$$\nabla \cdot \boldsymbol{u} = 0 \tag{1}$$

$$\frac{D\boldsymbol{u}}{Dt} = -\frac{1}{\rho}\nabla \boldsymbol{P} + \nabla \cdot (\nu \nabla \boldsymbol{u}) + \boldsymbol{g} + \frac{\boldsymbol{f}}{\rho} \tag{2}$$

2.1.2 Temperature analysis

The governing equation for the temperature analysis is the heat conduction equation shown in Eq.3. where C_p is the specific heat at constant pressure, T is the temperature at the calculation point, and k is the thermal conductivity.

In the temperature analysis, this equation was discretized and solved using the high-precision MPS method as in the fluid analysis.

$$\rho C_p \frac{DT}{Dt} = k\nabla^2 T \tag{3}$$

2.2 Magnetic field analysis

As described in the previous chapter, the magnetic field analysis used the magnetic moment method[9], which does not require setting air calculation points or boundary conditions.

Consider a source in space with a magnetization of $\boldsymbol{M}$ (T), and consider the magnetic field intensity $\boldsymbol{B_c}$ (T) at an arbitrary point P at a distance $\boldsymbol{r}$ (m) away from it. In this case, when the magnetization $\boldsymbol{M}$ is constant in a closed domain**V**, the magnetic field intensity $\boldsymbol{B_c}$ created by the magnetization $\boldsymbol{M}$ in the closed domain **V** at any point P can be calculated as follows. (Eq.4)

$$\boldsymbol{B_c} = -\frac{1}{4\pi}\nabla\left\{\int_V \boldsymbol{M}\cdot\nabla\left(\frac{1}{r}\right)dV\right\} + M_P \tag{4}$$

However, M_P is as follows (Eq.5)

$$\boldsymbol{M_P} = \begin{cases}\boldsymbol{M}\ (\boldsymbol{P}\in\boldsymbol{V})\\ \boldsymbol{0}\ (\boldsymbol{P}\notin\boldsymbol{V})\end{cases} \tag{5}$$

Then by calculating the sum of the magnetic field contributions from all magnetic elements (each volume V_i) the magnetic flux density **B** at any point in that space can be calculated as follows (Eq.6)

$$\boldsymbol{B} = \boldsymbol{B_C} - \frac{\boldsymbol{1}}{\boldsymbol{4\pi}}\sum_{\boldsymbol{i=1}}^{\boldsymbol{n}}\boldsymbol{\nabla}\int_{\boldsymbol{V_i}}\boldsymbol{M_i}\cdot\boldsymbol{\nabla}\left(\frac{\boldsymbol{1}}{\boldsymbol{r_i}}\right)\boldsymbol{dV_i} \tag{6}$$

However, $\boldsymbol{M_i}$ is the magnetization in each magnetic element, and the magnetic field of the system can be calculated by superimposing the magnetization of each magnetic element and the magnetic field created by the source. However, each magnetic field cannot be calculated explicitly because the magnetizations excited within a magnetic body interact with each other. Therefore, we consider that the magnetization generated within a magnetic body is the magnetization generated by adding the effect of the magnetization of each element to the magnetization within an element of a magnetic body. Based on the above, the following integral equation (Eq.7) is solved to show the effect that magnetic element i receives from magnetic body j with volume V_i.

$$\boldsymbol{M_i} - \frac{\boldsymbol{\chi}}{\boldsymbol{4\pi}}\sum_{\boldsymbol{i=1}}^{\boldsymbol{n}}\boldsymbol{\nabla}\left\{\int_{\boldsymbol{V_j}}\boldsymbol{M_j}\cdot\boldsymbol{\nabla}\left(\frac{\boldsymbol{1}}{\boldsymbol{r_{ij}}}\right)\boldsymbol{dV_j}\right\} = \boldsymbol{\chi B_{ci}} \tag{7}$$

2.3 Viscosity calculation

The viscosity coefficient of molten resin, μ , is obtained by applying the shift factor of temperature based on the W.L.F. rule[10] to the power-law model[11] as shown in Eq.8 and Eq.9[12] where a_T is the shift factor of temperature, μ_0 is the viscosity coefficient when the shear rate is set to 0 m/s, $|\dot{\gamma}|$ is the shear rate, n is a power number, T is the temperature of the melted resin, T_s is the reference temperature, and C_1 and C_2 are parameters. The shear rate $|\dot{\gamma}|$ is obtained using the deformation rate tensor $\boldsymbol{D}$ as in Eq.10. The deformation velocity tensor $\boldsymbol{D}$ is obtained using the velocity gradient $\nabla\boldsymbol{u}$ as in Eq.11. Dividing the obtained viscosity coefficient

μ by the density ρ as in Eq.12 yields the kinematic viscosity coefficient ν,which is substituted into the kinematic viscosity coefficient ν in Eq.2 to combine the fluid analysis and temperature analysis.

$$\boldsymbol{\mu = a_T \mu_0 |\dot{\gamma}|^{n-1}} \tag{8}$$

$$\boldsymbol{a_T = exp\left[-\frac{C_1(T - T_s)}{C_2 + T - T_s}\right]} \tag{9}$$

$$\boldsymbol{|\dot{\gamma}| = \sqrt{2D:D}} \tag{10}$$

$$\boldsymbol{D = \frac{1}{2}\{\langle \nabla u \rangle + \langle \nabla u^T \rangle\}} \tag{11}$$

$$\boldsymbol{\nu = \frac{\mu}{\rho}} \tag{12}$$

2.4 Coupling methods

The injection molding process of bonded magnets was modeled by dividing it into four categories: injection, compression, magnetization, and cooling and hardening, as shown in Fig. 1. Injection and compression are simulated by making the molten resin flow from the inflow boundary in the fluid analysis. Magnetization was simulated by magnetizing the molten resin in the magnetic field analysis. Cooling was simulated by obtaining the temperature of the molten resin through temperature analysis. Curing was simulated by setting the velocity of the molten resin to 0 m/s when the resin cools and reaches a certain temperature.

Fig. 2 shows a flowchart of the analysis of the injection molding of a bond magnet. Temperature analysis, magnetic field analysis, and fluid analysis are performed in this order. Injection molding of a bonded magnet is simulated by the following procedure.

[1] Obtain each initial value.
[2] Update the temperature of the molten resin using temperature analysis.
[3] Calculate the magnetization of the molten resin and the magnetic force acting on the molten resin using magnetic field analysis.
[4] Perform a fluid analysis using the viscosity coefficient and magnetic force to update the position of the molten resin.
[5] Update the viscosity coefficient of the molten resin based on the updated temperature and shear rate.

Repeat steps [2] to [5] until the analysis is completed.

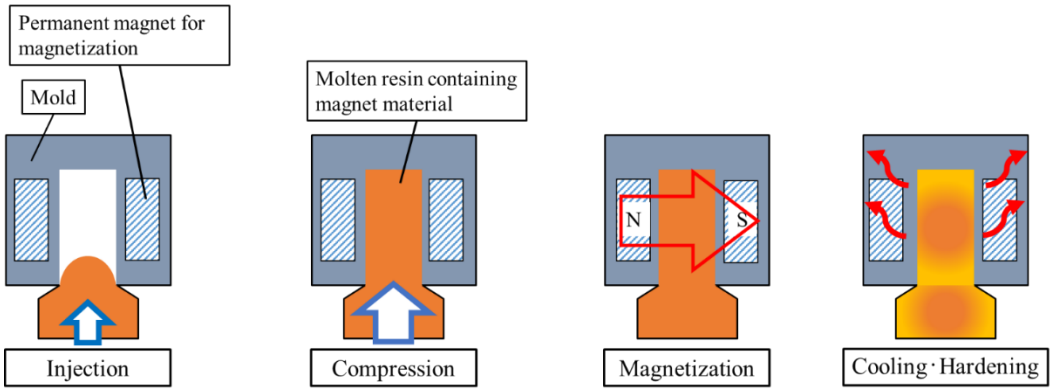

Figure 1: Injection molding process of bonded magnet.

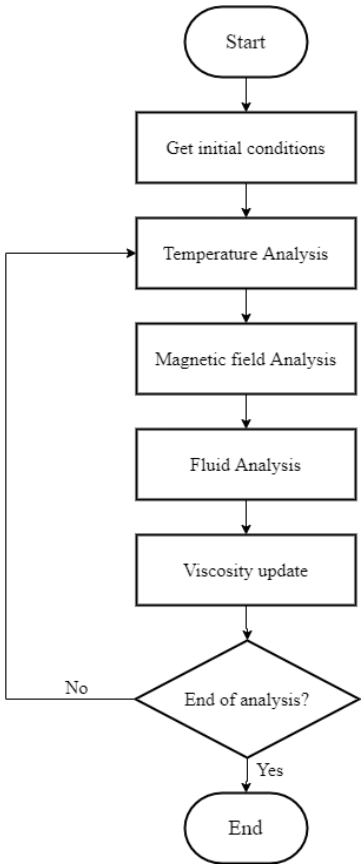

Figure 2: Flowchart of analysis.

3 ANALYSIS MODEL

3.1 Mold shape and dimensions

Fig. 3 shows the mold conditions. The mold was modeled so that the finished injection-molded product would be 10 mm × 4 mm × 80 mm (Fig. 3, red area). The molten resin is

injected from the left side of Fig. 3. The molten resin flows into the mold from the gate in the direction of the orange arrow from the left side of Fig. 3. The xy-section of the gate was modeled as 4 mm × 2 mm. The temperature measurement points for graphing the analysis results are indicated by light blue dots. There are four magnets (10 mm × 19 mm × 19 mm) for magnetization. The magnetizing magnets are arranged as shown in green on the upper side of Fig. 3. The direction of magnetization of the magnetization magnets is indicated by yellow arrows in Fig. 3. The direction of magnetization of the magnets is indicated by yellow arrows in Fig. 3.

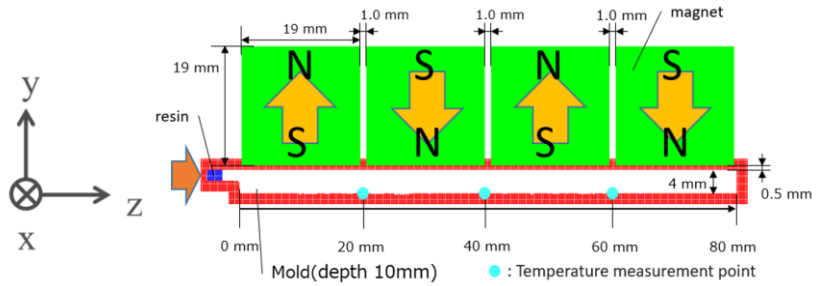

Figure 3: Mold conditions

3.2 Analysis conditions

The analysis conditions are as follows.

Table 1: Analysis conditions

Initial distance between particle [mm]	0.25
Initial particle number density [/mm^3]	26
Initial time interval [s]	1.0×10^{-5}
Density of molten resin [kg/m^3]	3650
Initial viscosity coefficient of molten resin [Pa･s]	160
Thermal conductivity of molten resin [W/(m･K)]	1.02
Melting point of resin [℃]	180
Relative permeability of molten resin	1.07
Density of the mold [kg/m^3]	7480
Thermal conductivity of the mold [W/(m･K)]	16.3
Specific heat of the mold [J/(kg･K)]	500
Magnetization of magnet [T]	1.1
Temperature of molten resin at the injection gate [℃]	300
Temperature of the mold [℃]	80
Injection speed [m/s]	2.5

4 VERIFICATION OF SKIN LAYER FORMATION PROCESS

This chapter clarifies the skin layer formation process in this simulation by comparing the

results of temperature analysis with the behavior of particles on the mold surface.

4.1 Temperature history

Fig. 4 shows the temperature history of the analysis results. Although there is a gradual decrease in temperature overall, a moment of rapid temperature increase can be observed at the 40 mm point. In the subsequent sections, the trend of particles on the mold surface at this particular point will be examined in detail.

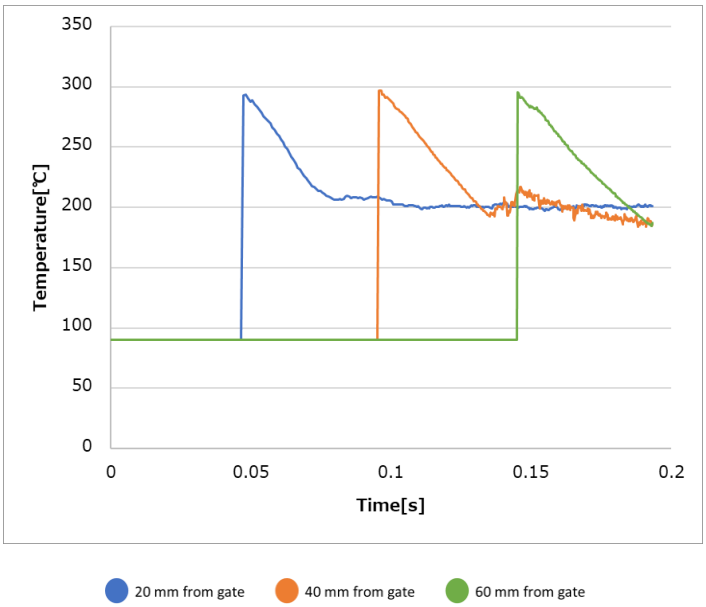

Figure 4: Temperature history.

4.2 Skin layer formation process

As described in the previous section, a temperature rise can be seen in a portion of the temperature history at the 40 mm point, as indicated by the red circle in Fig. 4. The behavior of the resin in this area is shown in Fig. 5. First, as shown in Fig. 5 (a), the particles in contact with the mold dissipate heat and the temperature of the resin falls and as shown in Fig. 5 (b), the resin that has reached the solidification temperature solidifies and adheres to the mold. Next, as shown in Fig. 5 (c), a gap is created between the resin that has solidified and remains in place and the resin that continues to flow without solidifying. This phenomenon is called "skin layer cracking" in the text. As shown in Fig. 5 (d), relatively hot resin penetrates into the cracks in the skin layer. The temperature rise is considered to be caused by the above phenomenon occurring at the 40 mm point. It is highly likely that this cracking of the skin layer also occurs as a real phenomenon.

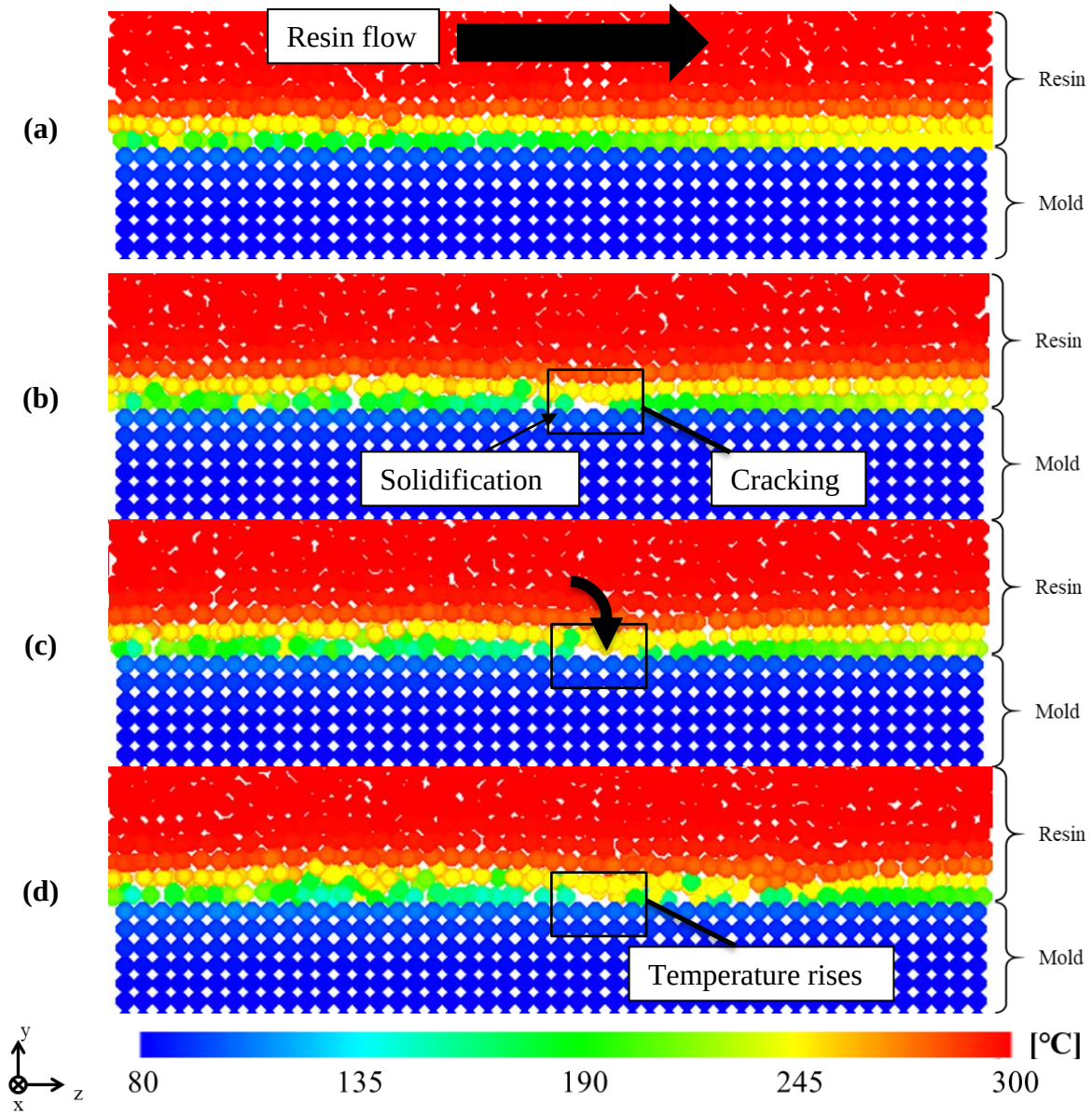

Figure 5: Snapshot of skin layer cracking.

5 SUMMARY

In this study, he were able to follow the detailed behavior of skin layer cracking during the skin layer formation process in injection molding into a rectangular mold by using a coupled analysis method based on the particle method. In the future, he will further elucidate the behavior of skin layer formation and its effect on molded products through comparison with actual equipment and analysis of different geometries and injection conditions.

REFERENCES

[1] Shimoda, T., "Current Status and Future of Rare Earth Bonded Magnets", Powder and

Powder Metallurgy, Vol. 40, No. 9.
[2] Koshizuka, S., Shibata, K., Muroya, K., "Introduction to Particle Methods: From Basics of Fluid Simulation to Parallel Computation and Visualization with C/C++ Source Code", Maruzen Publishing, 2014.
[3] N. Takahashi and T. Nakata, Optimal design method of 3-D nonlinear magnetic circuit by using magnetization integral equation method, IEEE Trans. on Magn., Vol. 25, No.5, pp. 4144-4146, Sep. 1989.
[4] Kitamura, T., "Elucidation and Visualization of the Injection Molding Mechanism of Bonded Magnets", Master's Thesis, Graduate School of Engineering, Osaka University, 2021.
[5] A. Khayyer and H. Gotoh, Modified Moving Particle Semi-implicit methods for the prediction of 2D wave impact pressure, Coastal Engineering, Vol. 56, No. 4, pp. 419-440, 2009
[6] A. Khayyer and H. Gotoh, Enhancement of stability and accuracy of the moving particle semi-implicit method, Journal of Computational Physics, Vol. 230, No. 8, pp. 3093-3118, 2011
[7] M. Kondo and S. Koshizuka, “Improvement of stability in moving particle semi-implicit method”, International Journal for Numerical Methods in Fluids, Vol. 65, No. 6 (2011), pp. 638-654
[8] Goto, H., "Particle Methods: Computational Science for Continua, Multiphase Flows, and Granular Media", Morinorth Publishing, 2018.
[9] Kofuji, K., Hirata, K., Miyasaka, F., Matsuzawa, S., "Analysis of Electromagnetic Phenomena by Coupling Particle Methods and Magnetic Moment Methods", Journal of the Japan Society of AEM, Vol. 23, No. 2, 2015.
[10] M. L. Williams, R. F. Landel and J. D. Ferry, “The Temperature Dependence of Relaxation Mechanisms in Amorphous Polymers and Other Glass-forming Liquids”, Journal of the American Chemical Society, Vol. 77, No. 14 (1955), pp. 3701-3707
[11] Fukuzawa, Y., Tomiyama, H., Shibata, K., Koshizuka, S., "Flow Analysis of High-Viscosity Non-Newtonian Fluids Using the MPS Method", Transactions of the Japan Society of Computational Engineering and Science, Vol. 2014, 2014, p. 20140007.